PRÉCIS

This book contains a systematic development of the fundamentals of finite inelastic deformations of heterogeneous materials. It is a treatise aimed to provide a basic foundation for advanced graduate study and research in the mechanics of materials, including single crystal and polycrystal metals, and granular materials. A reader with minimal exposure to continuum mechanics and some vector and tensor calculus should be able to master the mathematical necessities that are covered in the first two chapters. An effort is made to provide sufficient detail in order to render the book accessible to students in analytical, computational, and experimental mechanics and the mechanics of materials.

To guide the reader, each chapter is preceded by a brief description of its contents. There are nine chapters, each divided into several sections and subsections. Many sections also begin with a brief description of their contents. Each chapter ends with a list of cited references.

As a foundation, the geometrical, kinematical, and dynamical ingredients are treated in Chapters 1, 2, and 3. For the most part, coordinate-independent vector and tensor notation is used. This however, is augmented by frequent component representation of various expressions in indicial notation, rendering the book accessible to a broader audience. The continuum theories of the rate-independent and rate-dependent deformation of metals and geomaterials (granular materials and rocks) are developed in Chapter 4, where, based on a general framework, many specific cases are detailed and explicit equations useful for computational simulations are given. Included in this chapter (Section 4.8) are detailed presentations of dislocation-based rate- and temperature-dependent models of metals, together with experimentally-obtained values of the corresponding constitutive parameters. Chapter 5 is devoted to techniques for the integration of continuum constitutive equations. Both rate-independent and rate-dependent deformations, including the effects of thermal softening, friction, and dilatancy, are considered. Included are forward-gradient integration techniques, as well as a more efficient technique based on a plastic-predictor/elastic-corrector method, recently developed by the author and his coworkers. Each computational method is described, computational steps are listed, and illustrative examples are provided, leading to a comparative evaluation of various methods. Chapter 6 contains the fundamentals of finite elasto-plastic deformation of single crystals, from a micromechanical point of view, starting with a review of the crystal systems and certain elementary topics in the theory of dislocations. Physically-based constitutive relations for single crystals are formulated in this chapter on the basis of slip-induced plastic deformation and the accompanying elastic lattice distortion. The notions of self- and latent-hardening are critically examined, and slip models which directly account for both the temperature- and strain-rate effects, are presented and applied to predict the polycrystal flow stress of both bcc (commercially pure tantalum) and fcc

(OFHC copper) metals over a broad range of strains, strain rates, and temperatures. Chapter 7 covers the micromechanics of finite elastoplastic deformation of densely-packed granular materials. Here, physically-based constitutive relations are developed for particulate materials that carry the applied loads through frictional contacts, based on the slip- and rolling-induced (anisotropic) inelastic deformation, accompanied by shear-induced and pressure-dependent inelastic volumetric changes. In Chapter 8 the mathematical foundation of the transition from micro to macro variables is laid out. Exact results on averaging techniques, valid at finite deformations and rotations, are developed, giving explicit equations for the calculation of the generalized Eshelby tensor and its conjugate, within a nonlinear finite-deformation setting. Aggregate properties and averaging *models* are presented in this chapter, including the Taylor, the self-consistent, and the double-inclusion models. Special advanced experimental methods are reviewed in Chapter 9, and some typical experimental results on large strain, high strain-rate deformation of several metals are given. Included also are experimental results on the deformation and shearbanding of cohesionless frictional granular materials. What follows is a more detailed description of the contents of each chapter.

Chapter 1 includes a treatment of second-order tensors, tensor equations, and a class of isotropic functions of second-order tensors. Both spectral (Sections 1.2 and 1.3) and coordinate-independent (Section 1.5) representations are given. A number of important identities (Section 1.4) are developed, which are then used throughout the book. Tensors and a class of tensor-valued functions with distinct real or complex eigenvalues, as well as cases with repeated eigenvalues, are examined in detail, providing explicit equations which are then used throughout the book. The time derivative of tensor-valued isotropic functions of a time-dependent, second-order tensor, is considered in Section 1.6. Again, cases with distinct and repeated eigenvalues are studied in detail. These results provide powerful tools for computational algorithms, and this is discussed and illustrated, in Chapter 5.

Chapter 2 is devoted to the kinematics of finite deformations and rotations. After a brief review of the basic elements of the kinematics of deformation and its description in Lagrangian and Eulerian triads (Section 2.1), and polar decomposition (Section 2.2), a comprehensive account of various strain measures (Section 2.3), their rates and the associated spin tensors (Sections 2.4 and 2.5), is provided. Various measures of the material spin are examined in Section 2.6. In Sections 2.7 and 2.8, the relations between the deformation-rate and the stretch tensors are examined, and in Section 2.9, relations among various spin tensors are outlined. Section 2.10 is devoted to an examination of various strain rates and the manner by which they relate to one another. Both spectral representation and coordinate-independent expressions are given. Relations among strain measures, strain-rate measures, and spin tensors are detailed.

A discussion of the stress and stress-rate measures, and the balance relations are contained in Chapter 3. Various stress measures, conjugate to the strain measures developed in Chapter 2, are worked out in detail and the relations among them are established (Sections 3.1 and 3.2). Then, stress-rate measures are developed and general relations connecting the objective stress rates are presented (Sections 3.4 and 3.5). Balance relations and boundary-value

problems are briefly formulated (Section 3.6), together with the principle of virtual work (Section 3.7), relevant to nonlinear finite-deformation problems. This chapter also includes a weak form of the equations of motion, for application to a finite-element formulation of finite-deformation problems (Section 3.8). Explicit finite-element equations are developed and several important issues are clarified. Other topics discussed in this chapter are the kinematics, dynamics, and balance relations at surfaces of discontinuity (Section 3.9). Finally, the chapter includes a comprehensive account of general variational principles for finite deformation of hyperelastic materials, as well as the corresponding incremental and linearized formulations (Section 3.10).

The continuum theories of elastoplasticity are developed in Chapter 4, beginning with a discussion of the thermodynamics of inelasticity (Section 4.1), elastic and inelastic potentials, and the normality rule. Then, rate-independent theories of plasticity, with both smooth yield surfaces (Section 4.2) and yield surfaces with corners (vertex models, Section 4.4) are presented in a general setting, in terms of an arbitrary strain measure and its conjugate stress measure. Based on this, several commonly used plasticity models with isotropic, kinematic, and combined isotropic-kinematic hardening, are developed, and explicit equations useful for computational implementation, are given in various subsections of Section 4.2. The questions of dilatancy, pressure-sensitivity, friction, and their constitutive modeling are examined in some detail (Section 4.3), providing specific illustrative examples and comparisons with experimental results. The often-used deformation theories of plasticity are also examined, starting from nonlinear elasticity and systematically leading to the vertex model of elastoplasticity (Section 4.5). Another topic covered in this chapter is the physical basis of the noncoaxiality of the plastic strain rate and the deviatoric stress (Section 4.6). As is shown, this property is an integral part of the response of all frictional materials (Section 4.7). In this sense, the non-Schmid effects for crystal plasticity and pressure-sensitivity and frictional effects in the deformation of granular materials, are formulated in a unified manner, seeking to make the vast literature available in these two, seemingly unrelated, scientific inquiries, equally accessible to students and researchers interested in metal plasticity and/or the inelastic deformation of geomaterials. The chapter includes both rate-dependent and rate-independent theories. The rate- and temperature-dependent models are examined in some detail in Section 4.8. First, several empirical models are discussed. Then, based on the mechanisms of plastic deformation by the motion of dislocations, physically-based models for the inelastic deformation of bcc and fcc metals are developed and used to predict the flow stress of commercially pure tantalum, molybdenum, niobium, vanadium, several steels and titanium alloys, and OFHC copper, over a broad range of strains, strain rates, and temperatures, arriving at excellent correlation with experimental results with few free constitutive parameters. These parameters are then tabulated. This chapter also includes a detailed development (Section 4.9) of general continuum anisotropic elastoplasticity in terms of the decomposition of the deformation gradient into an elastic and a nonelastic contribution. It is shown that such a decomposition can always be reformulated and reduced to a (unique) purely inelastic and a (unique) purely elastic constituent that involves no rigid-body rotation, and an accompanying (unique) rigid-body rotation. Objective spin tensors associated with elastic and inelastic strain rates are

identified and formulae are given which explicitly express these spins as linear and homogeneous functions of the corresponding deformation rates. Included in this section is the examination of the requirements of the material frame indifference, the general elastic response in terms of an elastic potential, and a detailed description of how various rate quantities can be calculated explicitly, once the elastic potential and the constitutive relations for the plastic strain-rate tensor are given. Several, commonly misunderstood issues in finite inelastic deformations of continua, are critically examined and correct results are given, emphasizing some of the inherent difficulties with the treatment of anisotropic elastoplasticity in terms of the decomposition of the total deformation gradient into elastic and nonelastic parts. Small elastic deformations and very small elastic strains are also considered as special cases. Also discussed are the notion of the backstress and its objective time rate of change, as well as an alternative additive decomposition of the total deformation gradient.

Chapter 5 addresses the question of the integration of continuum constitutive equations, which plays a central role in computational modeling and numerical solutions of finite-deformation problems. The aim is to provide a solid footing for the development of constitutive algorithms which have the necessary accuracy, stability, and efficiency, for implementation into computational codes. After some brief historical comments in Section 5.1, the consequences of kinematical assumptions, such as the incrementally constant velocity gradient and the unidirectional stretch, are examined in detail and the exact coordinate-independent relation between the velocity gradient and the incremental deformation gradient is formulated (Section 5.2). For illustration of various constitutive algorithms, the J_2-flow theories of Chapter 4 are used, including both the rate-dependent and rate-independent cases, as well as the effects of thermal softening (Section 5.3). In Section 5.4, the mathematical basis of the recently proposed plastic-predictor/elastic-corrector method is outlined, and error estimates are given. Section 5.5 is devoted to a detailed account of the application of the singular perturbation method to solve the stiff constitutive equations which govern the variation of the stress magnitude. This section is closed by presenting a modified outer solution which is explicit, simple, accurate, and can be used directly in large-scale computations. Section 5.6 provides a detailed account of computational algorithms for proportional loading and unloading. In the algorithm, the deformation-rate tensor is assumed to remain codirectional with the stress-difference tensor which is defined as the deviatoric part of the Kirchhoff stress less the (deviatoric) backstress. Various integration methods are discussed, illustrated, and compared, for both the rate-dependent and rate-independent flow stress, considering loading as well as unloading. The computational steps are outlined in tables, through specific numerical examples. Computational algorithms based on the assumption of unidirectional stretch are examined in Section 5.7, and those based on the assumption of constant velocity gradient are detailed in Section 5.8. The results are compared for both rate-dependent and rate-independent cases, and their relative merits are discussed. The relation with the classical radial-return method is studied and generalized radial return techniques for application to the cases with large rotations, kinematic hardening, and noncoaxiality of the strain rate and stress, as well as cases with dilatancy and pressure-sensitivity, are formulated. For large deformations and the elastic-perfectly-plastic model, exact integration formulae are

presented and used to develop accurate and efficient algorithms, when the model includes workhardening and thermal softening, as well as noncoaxiality and other effects. Several useful tensorial identities are worked out in Appendices 5.A and 5.B, providing explicit exact results that can be directly implemented in large-scale numerical codes.

The elastoplastic deformation of single crystals is examined in Chapter 6. The chapter includes (Section 6.1) brief discussions of crystal structure, crystal plasticity based on dislocations and slip, and various topics in the dislocation theory, necessary for a fundamental understanding of the micromechanics of crystal deformation, including the characterization of dislocations, their elastic interactions which underlie certain aspects of strain hardening in metals, and other relevant issues. Section 6.1 is concluded by developing an explicit expression for a slip rate in terms of the density of the associated mobile dislocations, their average velocity, and the magnitude of the Burgers vector. The kinematics of the finite deformation of single crystals is addressed in Section 6.2. Various decompositions of the deformation gradient and its rate are discussed, providing detailed accounts of alternative representations of the deformation and spin tensors corresponding to various possible reference states. The elasticity of crystals is examined in Section 6.3, where explicit general rate-constitutive relations are presented, again using possible alternative reference states. Various objective stress rates are considered, the associated constitutive relations are produced, and their equivalence is established. The notions of self- and latent-hardening are critically examined in Section 6.4. The slip models which directly account for both the temperature- and strain-rate effects, are presented in Section 6.5. The short- and long-range barriers that the dislocations must overcome in their motion, are identified. The hardening issue of the rate-independent models in light of the short- and the long-range resistance to the motion of the dislocations is reexamined. Explicit results for bcc and fcc crystals are produced, taking into account the temperature, strain rate, and the long-range hardening effects, and the results are illustrated using the experimental data of commercially pure tantalum and OFHC copper. For these crystal structures, general constitutive algorithms for crystal plasticity calculations are also presented, and illustrative examples are given. As in Chapter 4, Section 4.8, dislocation-based crystal plasticity naturally involves several length scales relating to the dislocation densities and various microstructural characteristics of the material. The developed constitutive relations for crystalline slip, explicitly include three such length scales, directly related to the metal's microstructure. These results are new, and unrelated to the continuum gradient plasticity theories that are also briefly examined at the end of Section 6.5, together with couple-stress theories, size- versus length-scale effects, and the classical continuously distributed dislocation theory. Several issues associated with the microscopic (*i.e.*, at the dislocation and grain lengths) and continuum strain gradients are critically reviewed, and an attractive dislocation-based gradient model is produced that is valid at large deformations and reflects the spatial variations in the dislocation activities corresponding to the crystal slip. In this section, it is emphasized that for a sample with only a few interacting crystals, geometric and textural incompatibilities must be explicitly addressed, as they may profoundly affect the overall sample response.

The fundamentals of finite elastoplastic deformation of densely-packed granular materials, are discussed in Chapter 7 from a microscopic point of view. In Section 7.1, an overview of the micromechanics of the flow of frictional granules is given, illustrating the controlling influence of the induced anisotropy or fabric on the accompanying dilatancy or densification. Stress measures are formulated in terms of the contact forces and the granular microstructure in Section 7.2, where the basic concepts associated with fabric anisotropy and fabric measures, relations between the stress and fabric measures, and, finally, the connection between the back stress and the induced fabric anisotropy are discussed in some detail. A number of fabric measures are then presented for densely-packed rigid spheres in Section 7.3. Experimental results on rod-like photoelastic granules, subjected to cyclic shearing, as well as to monotonically applied biaxial compression, are then examined in Section 7.4, and various fabric tensors are correlated with the corresponding stress and strain. The remaining part of this chapter is devoted to the kinematics and constitutive modeling of frictional granules. A unified constitutive formulation at the meso-scale is presented in Section 7.5, and some of its implications are discussed, including the close relation between the double-slip theory of single crystals and that of granular materials, and the generalization to three-dimensional constitutive relations. The resulting constitutive relations account for pressure sensitivity, friction, dilatancy (densification), and, most importantly, the fabric (anisotropy) and its evolution in the course of deformation. The presented theory fully integrates the micromechanics of frictional granular assemblies at the micro- (grains), meso- (large collections of grains associated with sliding planes), and macro- (continuum) scales. Illustrative examples are given with comparison with experimental results.

Chapter 8 is devoted to the development of the exact mathematical tools necessary for obtaining average quantities and the homogenization of heterogeneous elastoplastic materials at finite strains and rotations. The choice of deformation and stress measures and their rates is examined and it is shown that the deformation gradient and the nominal stress, as well as their rates, are particularly useful quantities, with a number of consequential averaging properties. A set of general identities valid at arbitrary strains and rotations, is provided in Section 8.1, and the resulting implications are discussed for uniform boundary tractions and traction rates, and linear boundary displacements and displacement rates. These identities are valid for both rate-independent and rate-dependent materials, whereas only the rate-independent materials are considered in Sections 8.2 to 8.6 and most of Section 8.7. In Section 8.2, it is shown how a homogenization formalism of linear elasticity, in terms of Eshelby's tensor and its conjugate, can be modified and applied to general finite-strain and finite-rotation problems, with exact, calculable results, provided that the rate of the deformation gradient and the nominal stress rate are used as the kinematical and dynamical variables. Homogenization with the aid of an eigenvelocity gradient and an eigenstress rate, is formulated, the consistency conditions are established, and concentration tensors for ellipsoidal inhomogeneities are given explicitly. Green's functions for the rate quantities are discussed in Section 8.3, and formulae for the calculation of the generalized Eshelby tensor and its conjugate are presented in a fully nonlinear finite-deformation setting, based on suitable rate kinematical and dynamical variables. The double- and multiple-inclusion

problems are discussed in Section 8.4. The connections among strong ellipticity, inception of localized deformations, and Green's function are discussed in Section 8.5. Appendix A of this chapter gives explicit formulae for the calculation of the Eshelby tensor in two dimensions. Selected homogenization models are discussed in Section 8.6 for general composites, and in Section 8.7 for polycrystals, where the application of the exact results to the problem of estimating the overall mechanical response of a finitely deformed heterogeneous representative volume element (RVE) is outlined and the overall effective pseudo-modulus tensor (or pseudo-compliance tensor) of the RVE is calculated for rate-independent elastoplastic materials. Included in this section are comments on the Sack's and Taylor's models, as well as the self-consistent and double-inclusion models.

A discussion of two classes of special experimental methods and some related experimental results are included in Chapter 9. The first class is for the characterization of the response of metals over a broad range of strains, strain rates, and temperatures, and the second is for the characterization of quasi-static deformation of frictional granules, supplementing the experimental techniques and results on the biaxial loading and simple shearing of photoelastic granules, presented in Section 7.4. After a brief historical account of the origin of the Hopkinson technique, the classical Kolsky bar method is examined in Section 9.1. Then, in Sections 9.2 and 9.3, some recent novel Hopkinson techniques that allow for recovery experiments at various strain rates and temperatures, are discussed in detail. By these techniques it is possible to obtain the isothermal, as well as adiabatic, flow stress of many metals at high strains over a broad range of temperatures and strain rates. This is discussed and illustrated in terms of the experimental data that are given in Sections 4.8 and 6.5 of Chapters 4 and 6, for copper, tantalum, molybdenum, niobium, vanadium, titanium, and steels. Included in Section 9.3 are techniques for direct and indirect measurement of the fraction of work that is used to generate heat within the material, at high strain rates and for large plastic deformations. Section 9.4 details a new triaxial Hopkinson technique that allows simultaneously subjecting a sample to axial and lateral pressures at various strain rates. Finally, the chapter includes a detailed discussion of the triaxial deformation of cohesionless saturated granular materials, and X-ray techniques recently developed to monitor the deformation and the resulting shearbands in cyclic shearing under confining pressure, for this class of materials. Experimental results on densification of drained samples and liquefaction of saturated undrained samples are also presented in Section 9.5, and in Section 9.6, the X-ray techniques are discussed and illustrative results are given.

1

GEOMETRY

This chapter includes some basic topics in three-dimensional tensors and tensor-valued functions. Second-order tensors and certain arbitrary functions of second-order tensors are considered. These are basic in the description of the kinematics of finite deformation. In addition, time-derivatives of time-dependent second-order tensors and their tensor-valued functions are developed in coordinate-independent form. For clarity in presentation, components with respect to a fixed rectangular Cartesian coordinate system are also considered. While the derivation of the results utilizes eigenvectors and their reciprocals, the final expressions are given in direct coordinate-independent form.

More specifically, the notation is introduced in Section 1.1, and the spectral representation of second-order tensors is reviewed in Section 1.2, where formulae for calculating the eigenvalues of second-order tensors are summarized. In Section 1.3, oblique coordinates are considered, reciprocal base vectors are introduced, and spectral representations of second-order tensors and their integral powers are summarized. In these sections, cases with distinct and repeated eigenvalues are examined separately. Both symmetric and nonsymmetric real-valued tensors are examined, including cases with complex-valued eigenvalues and eigenvectors. Section 1.4 provides a set of identities for second-order tensors and gives the solutions to some useful linear tensor equations. These results provide tools for later application throughout the book. Certain isotropic tensor-valued functions of a second-order tensor are examined in Section 1.5, including a detailed study of cases where the tensor-valued argument may admit distinct or repeated eigenvalues. When the tensor argument depends on a scalar variable, say, time, its derivative and the time derivative of its isotropic functions are considered in Section 1.6, providing explicit coordinate-independent expressions for these derivatives. The material in this chapter serves as a background for the topics that are covered later on.

A reader new to the field of continuum mechanics may wish to read Sections 1.1 and 1.2 with care and then move to Chapter 2, using the remaining sections of this chapter as reference material.

1.1. NOTATION

For simplicity, a background fixed rectangular Cartesian coordinate system is used; see Figure 1.1.1. The unit coordinate base vectors are denoted by $\mathbf{e}_1$, $\mathbf{e}_2$, and $\mathbf{e}_3$. Both subscript and direct notation are used throughout. Depending on the occasion, the unit coordinate triad, ($\mathbf{e}_1$, $\mathbf{e}_2$, $\mathbf{e}_3$), is collectively denoted by $\mathbf{e}_i$ or $\mathbf{e}_A$ or $\mathbf{e}_a$, i, A, a = 1, 2, 3. Vectors are generally designated by bold-face letters, such as **a**, **b**, which have the representation $\mathbf{a} = a_i\,\mathbf{e}_i$, $\mathbf{b} = b_j\,\mathbf{e}_j$ with respect to the $\mathbf{e}_i$-triad, where $a_i = \mathbf{a}\cdot\mathbf{e}_i$ and $b_j = \mathbf{b}\cdot\mathbf{e}_j$. Here and throughout, the scalar product of two vectors is denoted by a dot between them, and the summation convention on repeated indices is used. For example, the scalar product of real-valued vectors **a** and **b** is[1]

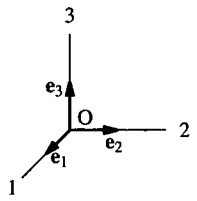

Figure 1.1.1

Rectangular Cartesian coordinates with corresponding unit base vectors

$$\mathbf{a}\cdot\mathbf{b} = (a_i\,\mathbf{e}_i)\cdot(b_j\,\mathbf{e}_j) = a_i\,b_j\,\mathbf{e}_i\cdot\mathbf{e}_j = a_i\,b_j\,\delta_{ij} = a_i\,b_i$$
$$= a_1\,b_1 + a_2\,b_2 + a_3\,b_3\,, \tag{1.1.1a}$$

where the *Kronecker delta* is defined by

$$\mathbf{e}_i\cdot\mathbf{e}_j = \delta_{ij} = \begin{cases} 1 & \text{when } i = j \\ 0 & \text{when } i \neq j \end{cases}. \tag{1.1.1b}$$

If the magnitude of **a** is a, and that of **b** is b, then $\mathbf{a}\cdot\mathbf{b} = a_i\,b_i = a\,b\cos\theta$, where θ is the angle between the two vectors.

The cross product of **a** and **b** is a vector **c** normal to their plane, forming a right-handed triad with them, and having magnitude $a\,b\sin\theta$. The cross product of the base vectors $\mathbf{e}_i$ and $\mathbf{e}_j$ is

$$\mathbf{e}_i\times\mathbf{e}_j = e_{ijk}\,\mathbf{e}_k\,, \quad i, j, k = 1, 2, 3\,, \tag{1.1.2a}$$

where the permutation symbol e_{ijk} equals (+1, −1, 0) depending on whether ijk forms (even, odd, no) permutation of 1 2 3. Then

$$\mathbf{a}\times\mathbf{b} = a_i\,b_j\,e_{ijk}\,\mathbf{e}_k\,. \tag{1.1.2b}$$

An ordered pair of vectors, written as $\mathbf{a}\otimes\mathbf{b}$, forms a second-order tensor with the following coordinate representation:

$$\mathbf{a}\otimes\mathbf{b} = a_i\,b_j\,\mathbf{e}_i\otimes\mathbf{e}_j\,. \tag{1.1.3}$$

[1] Mostly, vectorial and tensorial quantities are real-valued. However, complex-valued quantities are also considered when necessary, *e.g.*, complex-valued eigenvectors of real-valued second-order tensors, as in Subsection 1.3.7.

1.1.1. Contraction

When a general second-order tensor $\mathbf{T}$ with components T_{ij} *operates* on a vector $\mathbf{n}$ with components n_i, a vector, say, $\mathbf{t}$, with components

$$t_i = T_{ij}\, n_j \tag{1.1.4a}$$

is produced. Throughout, *matrix operation rules are used,* so that (1.1.4a) also has the following *direct* (coordinate-independent) representation:

$$\mathbf{t} = \mathbf{T}\,\mathbf{n}\,; \tag{1.1.4b}$$

a second-order tensor followed by a vector implies *contraction.* The components of $\mathbf{T}$ are $T_{ij} = \mathbf{e}_i \cdot \mathbf{T}\,\mathbf{e}_j$. The notation $\mathbf{n}\,\mathbf{T}$ is also used for $\mathbf{n} \cdot \mathbf{T}$ which is a vector with components $n_i\, T_{ij}$. If $\mathbf{T} = \mathbf{T}(\mathbf{x})$ is a tensor-valued, differentiable function, its divergence is written as

$$\nabla\,\mathbf{T} \equiv \nabla \cdot \mathbf{T} = \left[\mathbf{e}_i \frac{\partial}{\partial x_i}\right] \cdot (T_{jk}\,\mathbf{e}_j \otimes \mathbf{e}_k) = (\partial\, T_{ij}/\partial x_i)\,\mathbf{e}_j\,. \tag{1.1.5a}$$

The tensorial operation of ∇ on $\mathbf{T}$ is represented by

$$\nabla \otimes \mathbf{T} \equiv (\partial\, T_{ij}/\partial x_k)\,\mathbf{e}_k \otimes \mathbf{e}_i \otimes \mathbf{e}_j\,. \tag{1.1.5b}$$

If $\mathbf{S}$ and $\mathbf{E}$ are two second-order tensors with respective components S_{ij} and E_{ij}, then the single and double contraction of their products, respectively, is a second-order tensor with components $S_{ij}\,E_{jk}$ and a scalar $S_{ij}\,E_{ji}$, as follows:

$$\mathbf{S}\,\mathbf{E} \equiv \mathbf{S} \cdot \mathbf{E} = S_{ij}\,E_{jk}\,\mathbf{e}_i \otimes \mathbf{e}_k$$

$$\mathrm{tr}\,(\mathbf{S}\,\mathbf{E}) \equiv \mathbf{S} : \mathbf{E} = S_{ij}\,E_{ji}\,. \tag{1.1.6a,b}$$

Similarly, if $\mathcal{L}$ is a fourth-order tensor with components $\mathcal{L}_{ijkl}$, then

$$\mathcal{L}\,\mathbf{E} \equiv \mathcal{L} : \mathbf{E} = \mathcal{L}_{ijlk}\,E_{kl}\,\mathbf{e}_i \otimes \mathbf{e}_j\,. \tag{1.1.7}$$

The reader should note the order of contractions in these expressions, since alternative conventions are used elsewhere in the literature.[2] The transpose of a tensor is designated by superscript T. For example, $\mathbf{E}^{\mathrm{T}} = E_{ji}\,\mathbf{e}_i \otimes \mathbf{e}_j$ has components E_{ji}, when the components of $\mathbf{E} = E_{ij}\,\mathbf{e}_i \otimes \mathbf{e}_j$ are E_{ij}.

1.1.2. Scalar and Dyadic Products of Complex-valued Vectors

Consider two complex-valued vectors $\mathbf{z}_1 = \mathbf{x}_1 + i\,\mathbf{y}_1$ and $\mathbf{z}_2 = \mathbf{x}_2 + i\,\mathbf{y}_2$, with $\mathbf{x}_1$, $\mathbf{y}_1$, $\mathbf{x}_2$, and $\mathbf{y}_2$ being real-valued vectors, and $\sqrt{-1} = i$. First, introduce the notion of the *simple product* of $\mathbf{z}_1$ and $\mathbf{z}_2$, as follows:

$$\mathbf{z}_1\,\mathbf{z}_2 \equiv (\mathbf{x}_1 + i\,\mathbf{y}_1) \cdot (\mathbf{x}_2 + i\,\mathbf{y}_2)$$

$$= (\mathbf{x}_1 \cdot \mathbf{x}_2 - \mathbf{y}_1 \cdot \mathbf{y}_2) + i\,(\mathbf{x}_1 \cdot \mathbf{y}_2 + \mathbf{y}_1 \cdot \mathbf{x}_2)\,. \tag{1.1.8a}$$

[2] Nemat-Nasser and Hori (1993, 1999), for example, use the convention $\mathcal{L} : \mathbf{E} = \mathcal{L}_{ijkl}\,E_{kl}\,\mathbf{e}_i \otimes \mathbf{e}_j$.